Circulation Features Associated with the Winter Rainfall Decrease in Southwestern Australia

ROBERT J. ALLAN AND MALCOLM R. HAYLOCK

Climate Impact Group, CSIRO Division of Atmospheric Research, Melbourne, Australia

(Manuscript received 12 September 1991, in final form 16 November 1992)

ABSTRACT

A study of atmospheric and oceanic circulation features in the wider Australian region is undertaken in an attempt to establish the cause(s) of the observed decrease in austral winter (JJA) rainfall over the southwestern portion of Western Australia. Basic regional analyses reveal that long-term mean sea level pressure (MSLP) at Perth, Western Australia, is negatively correlated with southwestern Australian rainfall in JJA over the period 1876–1989. This significant MSLP–rainfall relationship is also observed when using smoothed data series, which resolve a decadal–multidecadal signal embedded within a long-term fluctuation. The latter is punctuated by a downward (upward) rainfall (MSLP) trend over the last 50–60 years that is most pronounced since the mid-1960s.

Such relationships are examined further using Southern Hemisphere gridded MSLP, sea surface temperature (SST), and cloudiness data in the Australian sector during the period 1911–1989. On decadal to multidecadal time frames (MSLP bandpass-filtered in the 7–20-year band), MSLP is out of phase between the Australian continent and the high latitudes of the Southern Ocean. Alternations in the sign of MSLP anomalies over these regions are observed during wet and dry extremes in southwestern Australian JJA rainfall. This is suggestive of changes in the longwave pattern, and thus a propensity for modulation of frontal activity, in the Australian region. Some coherent variations are also seen in SST and cloudiness fields, with perhaps an indication that cloud patterns are more organized across the southwest in wet winters.

The long-term MSLP analyses (low-pass-filtered MSLP to remove frequencies less than 25 years) indicate the influence of a different forcing on the regional climate system. The dominant pattern that emerges is of MSLP anomalies that are out of phase between the south-southwest of Australia and to the southeast of New Zealand. Since 1911, the above configuration of anomalies across southern latitudes has evolved slowly from a negative/positive to a positive/negative alignment. During this period, simultaneous correlations between Darwin MSLP and southwestern Australian JJA rainfall have also changed, from coherent and significant to insignificant. This suggests that low-frequency fluctuations in the El Niño–Southern Oscillation (ENSO) phenomenon may have played a major role in this process.

It would appear that southwestern Australian JJA rainfall patterns are modulated by a long-term MSLP signal with a pronounced trend in recent decades that is punctuated by decadal–multidecadal MSLP pulses. These MSLP–rainfall relationships are associated with circulation fluctuations in Australian longitudes that may be linked to low-frequency characteristics of the ENSO phenomenon. However, wider Southern Hemisphere data have not yet been analyzed to test this hypothesis further. Interestingly, MSLP fields resolved in this study bear little resemblance to 2 × CO_2 MSLP simulations of enhanced greenhouse conditions in any of the low- or high-resolution general circulation model (GCM) intercomparisons over the Australian region.

1. Introduction

In the last 20 years, a number of studies have detailed long-term decreases in rainfall over the southwestern austral winter rainfall region of Western Australia (see Fig. 1) (e.g., Gentilli 1971; Wright 1971, 1974a,b; Pittock 1975, 1983, 1988; Sadler et al. 1988; Broadbridge 1989; Nicholls and Lavery 1992). This decrease is evident in the period since the 1930–40s during May to October (Pittock 1983), being most pronounced in the winter months of June to August over the southwestern region of the state (Pittock 1988). As a consequence of such observed changes, there is concern that the recent downward trend in rainfall may continue, and that it could be an indication of the influence of the enhanced greenhouse effect. Alternatively, the rainfall changes may be symptomatic of natural variability in the climate system. However, there has been no detailed study linking the above trends to possible changes in atmospheric and oceanic circulation features.

Of the above studies, those of Wright (1971, 1974a,b) remain the most detailed, as they have attempted to distinguish the dominant patterns and circulation changes responsible for synoptic-scale forcings during early [May, June, July (MJJ)] and late [August, September, October (ASO)] winter periods. Using

Corresponding author address: Robert J. Allan, CSIRO Division of Atmospheric Research, Station Street, Aspendale, Private Bag No. 1, Modialloc, Melbourne, Victoria, Australia, 3195.

rainfall data from 1876–1970 and synoptic charts for the 1950s–60s, Wright (1971, 1974a,b) has suggested that MJJ rainfall in southwestern Australia is dominated by organized convection associated with broad ascending motion and enhanced zonal flow at midtropospheric levels and near-surface winds from the northwest (Type 1). This pattern describes atmospheric conditions important in the development of moist inflow from more tropical latitudes, but becomes less frequent by ASO (Gentilli 1979). During ASO, rainfall in southwestern Australia tends to be linked more to frontal systems and unstable airstreams from the west-southwest of the continent (Type 2). In these analyses, a major shift in the long-term winter rainfall pattern from 1881–1910 to 1911–40 is suggested, in which MJJ (ASO) rainfall increased (decreased) with an increase (decrease) in Type 1 influences. The other change seems to have occurred in the period from 1911–40 to 1941–70, with MJJ rainfall having increased under a regime of increased Type 1 and decreased Type 2, and ASO rainfall having decreased under a regime of decreased Type 2 pattern. Given that the above are synoptic characteristics, and as this dynamical climatology study straddles Wright's (1974a,b) early and late winter periods, this paper aims to resolve broad aspects of these circulation features.

Recent research has indicated that an important influence on winter rainfall patterns over the central western portions of the Australian continent is the distribution of sea surface temperature (SST) in the central and eastern Indian Ocean (Nicholls 1989; Smith 1993; Drosdowsky 1993). A synoptic feature that is often linked dynamically with interactions between low-latitude Indian Ocean SST anomalies and the atmospheric circulation is the low- to midlatitude, northwest–southeast oriented cloud band and its associated tropical temperature trough. Although these features have received most attention in association with widespread rainfall events over central to eastern Australia (Tapp and Barrell 1984), they could provide a link between tropical SSTs and rainfall over southwestern Australia. The importance of the cloud bands to rainfall patterns across the central regions of Western Australia in autumn to early winter months has been established (Gentilli 1979), and a detailed climatology of the bands and their relationship with various oceanic and atmospheric variables over the period from 1979–83 has been produced (Kuhnel 1990). Although the latter study indicates that cloud bands linked to warm SSTs in the Indian Ocean south of Sumatra can influence rainfall in the southwest of Western Australia, they are not seen as a consistent autumn and winter rainfall-producing mechanism. It is not known whether the broad climatological pattern has changed sufficiently to shift the frequency and/or position of these bands during the historical record.

A number of papers have shown that the main cause of both interannual and longer-term climatic variability in much of Australasia is the El Niño–Southern Oscillation (ENSO) phenomenon (see reviews in Allan 1988, 1989, 1991; National Climate Centre 1988). Although strong ENSO events can affect all of Australia (National Climate Centre 1988; Allan et al. 1990; Zhang and Casey 1992), correlations with the ENSO using datasets covering the last 50–60 years are poor across the western margins of the Australian continent (P. A. Jones 1991). However, the prospect that low-frequency changes in ENSO on decadal–multidecadal and longer time frames (Allan 1991, 1993; Elliott and Angell 1988; Enfield 1988, 1989; Enfield and Cid 1991; Zhang and Casey 1992) may be related to major rainfall fluctuations in this region has not been evaluated fully.

The research described above provides the background for this investigation of the influence of large-scale atmospheric and oceanic features on the winter rainfall regime over southwestern Australia. This involves an initial consideration of correlations between JJA rainfall and local station mean sea level pressure (MSLP) series, and expands to encompass wider regional MSLP–rainfall relationships. Rainfall modulations on decadal–multidecadal and long-term, low-frequency (greater than 25 years) time scales are apparent in these analyses, and are investigated using MSLP, SST, and cloudiness data since 1911.

2. Data sources and methods

Monthly mean district and station rainfall data used in this paper were obtained from the Australian Bureau of Meteorology. District rainfall records were available from 1913; data for districts 8 to 10A covering the southwestern corner of Western Australia (shaded in Fig. 1) have been averaged to give an area mean for

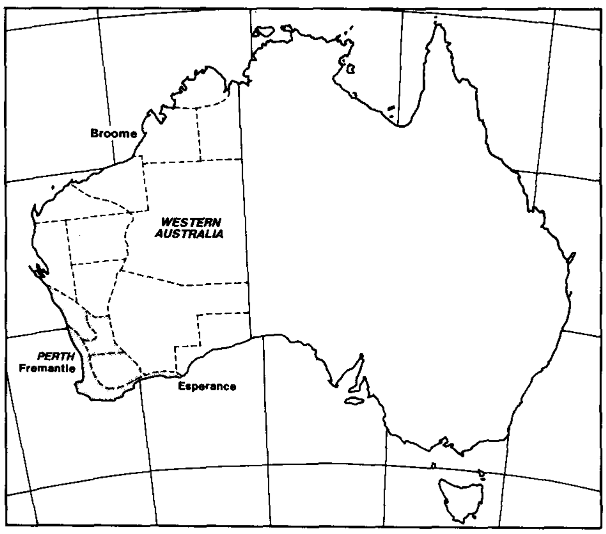

FIG. 1. Distribution of Western Australian rainfall districts, locations referred to in the text in Australia, and the southwestern region of Western Australia comprising districts 8 to 10A (shaded).

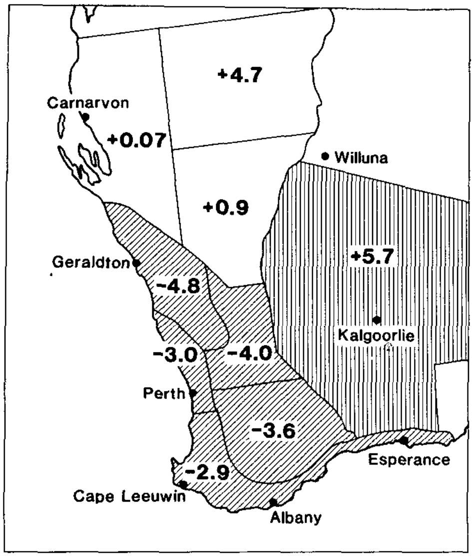

FIG. 2. Region of southwestern Australia showing the austral winter rainfall trends in percent per decade for rainfall districts over the period 1913–86. Shadings indicate trends that are statistically significant at the 95% confidence level (from Pittock 1988).

that region. This was done because of the consistent and significant downward trend in austral winter rainfall over these districts reported by Pittock (1988), and shown in Fig. 2. Prior to 1913, only rainfall records from individual stations are available. In order to obtain the longest record possible, an average of all long-term station rainfall data in the region encompassing districts 8 to 10A was compared with the average of the district rainfall. During the period of overlap since 1913, the regional rainfall patterns from the district and station averages were almost identical (not shown). A comparison with recent high-quality, long-term rainfall stations in southwestern Australia compiled by Lavery et al. (1992) showed very good agreement with the JJA rainfall series used in this study. Thus, average winter rainfall in southwestern Australia can be calculated from the 1870s using station data.

Monthly MSLP data for Perth since 1876 were assembled from Australian Bureau of Meteorology records. Earlier compilations by Cooke (1901), Lockyer (1908, 1909), Reseau Mondial (1910–34), Hunt (1929), and the Smithsonian Institute (1944) were also consulted because of apparent errors in the Australian Bureau of Meteorology compilation. The most obvious errors were related to a change in cistern height after 1967 and an apparent double correction made to the data during a cistern height change in the 1930s. Monthly MSLP data for Darwin since 1876 were assembled from a number of sources, and checked for inconsistencies (see details in Allan et al. 1991). Gridded monthly MSLP for the Australian sector of the Southern Hemisphere midlatitudes since 1911 were obtained from Fitzharris (1992, personal communication) and are described in P. D. Jones (1991). An intercomparison of this pressure set with a similar one from the Climate Research Division, Scripps Institution of Oceanography (Barnett and Jones 1992), suggests that they are almost identical when examined on large space–time scales. Problems appear to occur only with analyses of shorter-term (less than two years), small-region features. Monthly MSLP data for the Antarctic coastal stations at Halley Bay, SANAE, Novolazarevskaya, Molodezhnaya, Mawson, Davis, Mimy, Casey, and Dumont d'Urville were extracted from a dataset provided by the Carbon Dioxide Information Analysis Centre (CDIAC) and detailed in Jones and Wigley (1988) (Fig. 3).

Monthly mean total cloudiness data for the Indo-Australasian region were extracted from the global Comprehensive Ocean–Atmosphere Data Set (COADS) (Woodruff et al. 1987). Monthly mean historical sea surface temperatures (SSTs) in the Indo-Australasian region from 1854 to 1989 were obtained from the United Kingdom Meteorological Office (UKMO) (Parker 1987; Folland, 1992, personal communication). These data have recently been compiled in a global atlas by Bottomley et al. (1990).

Both austral winter monthly and seasonal means of the above atmospheric and oceanic parameters have been examined. The austral winter season was defined as June, July, and August (JJA). Monthly and JJA anomalies are deviations from the long-term 1911–89 mean. A running mean (seven point) was applied to the JJA Perth MSLP and southwestern Australian rainfall series in order to highlight both the long-term

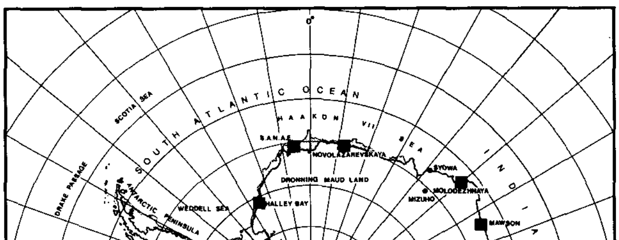

FIG. 3. Distribution of stations around the Antarctic coastal margin providing long-term mean sea level pressure (MSLP) data. Stations used are marked with a large solid square.

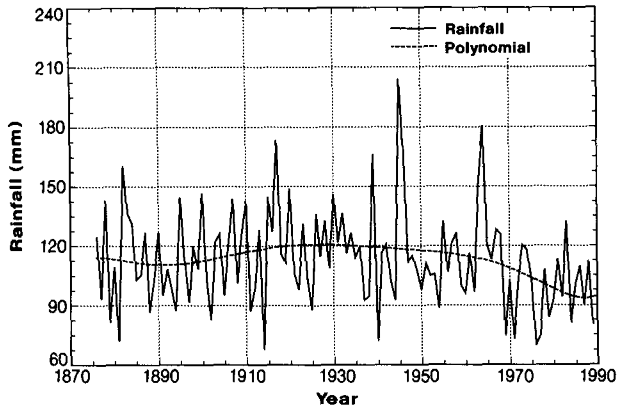

FIG. 4(a). Raw data and fitted curves of seventh-order polynomial of austral winter (JJA) southwestern Western Australian composited station rainfall (in districts 8 to 10A) over the period 1876–1989. Rainfall is given in mm.

trend and an apparent decadal–multidecadal signal in the data. The latter was resolved as being in the range of 7–20 years from a standard spectral analysis of the raw data series. Consequently, a recursive Butterworth (bandpass) filter (Stearns and Hush 1990) was applied to a detrended set (linear trend removed) of the southwest rainfall and gridded MSLP data, with high and low cutoff frequencies at 7 and 20 years, respectively, to extract the essence of the decadal–multidecadal feature. Composites of "wet" and "dry" winters used in this study were constructed by averaging the bandpass-filtered MSLP, SST, and cloudiness data for winters when bandpass-filtered rainfall was in the top and bottom quartiles of the range, respectively. The original gridded MSLP data were also subjected to a low-pass filter (Graham 1963) that suppressed frequencies higher than 25 years. This cutoff was used in order to maximize the low-frequency component in the data, while avoiding contamination that might arise from the 20–25-year "fringe" of the 7–20-year signal.

3. Results and discussion

One of the initial tasks in assessing the nature of the recent rainfall trend in southwestern Australia has been to determine whether similar trends are evident in the longer-term record, as suggested by the studies of Wright (1974a,b). JJA rainfall observations averaged over all available stations in southwestern Western Australia for the last 115 years (Fig. 4a) show the downward rainfall trend over the last 50 to 60 years, but also indicate that a period of relatively low rainfall occurred late last century. In contrast, during the first 30 to 40 years of this century, rainfall tended to be higher. Interestingly, regions immediately to the east-northeast (Fig. 2) show pronounced increases in rainfall in the 1913–86 period. This configuration is discussed in section 3c.

Analyses in Pittock and Allan (1990) and Allan et al. (1992) have suggested that large-scale, ocean–atmosphere circulation patterns are more likely to be the predominant influence on southwestern Australian rainfall than more localized warming effects from the poleward-flowing, near-coastal Leeuwin Current. Furthermore, long-term analyses of this feature are not possible, as data of the quality required to resolve the current are limited to the last decade or so. Consequently, in the following sections, long-term atmospheric and oceanic data are examined on regional scales in order to resolve the major features forcing the temporal behavior of rainfall in the region.

a. *Correlations with MSLP*

A basic atmospheric parameter that can be compared with the rainfall series is Perth MSLP, shown for the JJA period over the last 115 years in Fig. 4b. An examination of Figs. 4a and 4b shows that there is a strong inverse relationship between southwestern rainfall and Perth MSLP over the entire dataset (the correlation coefficient $r = -0.80$; $p < 1\%$).

To investigate the spatial representativeness of these signals, correlations between gridded MSLP data in the Australian region and southwestern rainfall from 1911 to 1989 are constructed for the individual months of June, July, and August (Figs. 5a–c). These fields indicate that winter rainfall in southwestern Australia is linked with MSLP variations over much of the continent. This is shown by the shaded regions in these diagrams (where positive and negative correlations are significant; $p < 1\%$). The most widespread and significant negative correlation pattern covers almost the entire continent and out into the southwestern Pacific in July. At high latitudes to the south-southeast of Australia, the correlations become significant and positive.

Spectral analyses (not shown) of the MSLP and

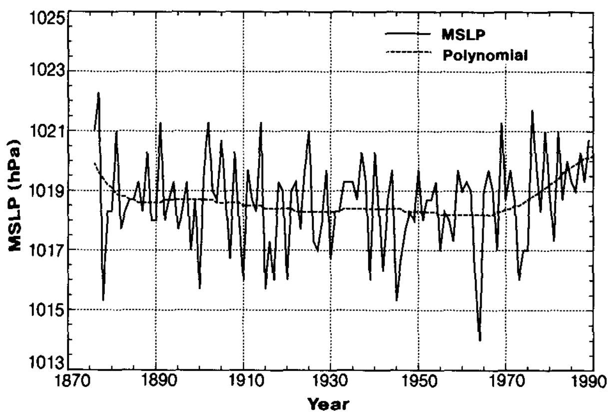

FIG. 4(b). Raw data and fitted curves of seventh-order polynomial of austral winter (JJA) Perth MSLP over the period 1876–1989. MSLP is in hPa.

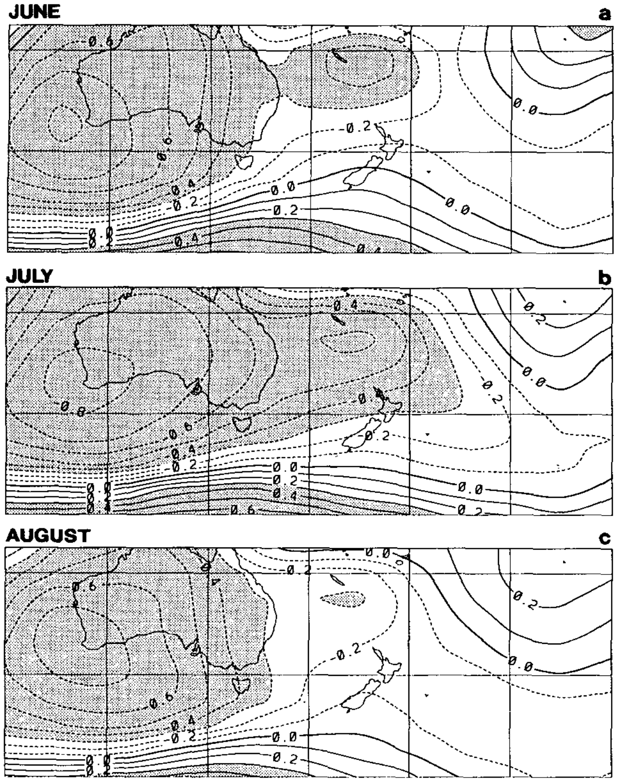

FIG. 5. (a) Correlation pattern between southwest Western Australian rainfall and gridded MSLP over Australasia in June for the period 1911–1989. Regions significant at the 99% confidence level are shaded. (b) As in Fig. 6a except for July. (c) As in Fig. 6a except for August.

rainfall series in Figs. 4a and 4b suggest that they also contain a decadal–multidecadal signal in the 7–20-year band. This can be seen in Fig. 6, where both series are subjected to a seven-point running mean, and found to be inversely correlated, with a coefficient of −0.64 ($p < 1\%$). The overall impression is of an MSLP–rainfall relationship that is marked by decadal–multidecadal fluctuations and a long-term, low-frequency signal that shows a very pronounced trend since the mid-1960s. In an effort to understand more about the structure of these features, gridded MSLP, SST, and cloudiness data over the wider Australasian region are bandpass-filtered in the 7–20-year range and low-pass filtered to capture low-frequency signals longer than 25 years.

b. Decadal–multidecadal signals in MSLP–rainfall relationships

From the bandpass-filtered analyses, wet winters are marked by a low pressure anomaly centered over and to the south-southwest of the continent, which extends a lobe southeastward beyond New Zealand, with the opposite pressure tendency in dry winters (Figs. 7a,b). These anomalies are out of phase with those associated with the core of the regional long-wave trough at higher southern latitudes. This configuration indicates that the winter cyclone tracks are displaced farther north in wet seasons and farther south in dry seasons. The pressure anomaly patterns for each of these composites show that anomalous westerly airflow occurs over southwestern Australia during wet periods, and anomalous easterly airflow during dry periods. Although examining circulation fluctuations on slightly longer time frames, Wright (1971, 1974a,b) noted a similar change. The bulk of the region in Figs. 7a,b is found to be statistically significant at the 95% level using a gridpoint t test, and 99.9% field significant using Monte Carlo methods.

Further details of the circulation on decadal–multidecadal time scales can be inferred from the wet and dry MSLP composites in Figs. 7c,d. When the high pressure center over the Australian continent is more intense, as in the dry winters (Fig. 7d), the low pressure trough at high latitudes to the south-southwest of Western Australia is stronger; the reverse occurs in wet winters (Fig. 7c). A similar relationship has been found at the 500-hPa level by Kidson (1988). It also seems to be the dominant signal in the gridded MSLP–rainfall correlation analyses in Fig. 5.

The most important feature of this link between MSLP and winter rainfall is that increases in MSLP over southwestern Australia in dry JJAs are a result of a westward, longitudinal expansion of the continental anticyclone. This association suggests a dynamical influence on rainfall patterns through circulation changes. During wet periods, the continental anticyclone is weaker and concentrated over central southern Australia, which together with higher MSLP in the long-wave trough, results in weaker zonal westerly air-

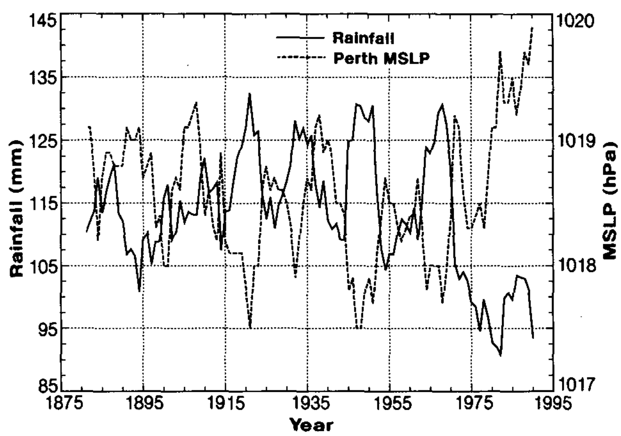

FIG. 6. Intercomparison of seven-point running-mean southwest Western Australian composited station rainfall and Perth MSLP during austral winter (JJA) from 1876–1989. Rainfall is given in mm and MSLP in hPa. The correlation coefficient between these data (−0.64) is statistically significant at the 99% level.

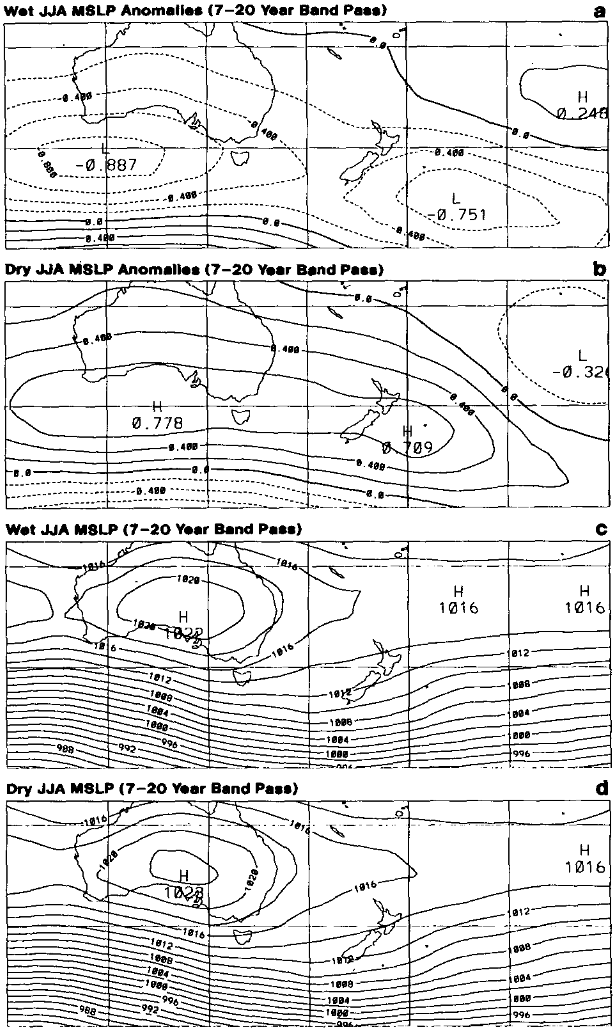

FIG. 7. (a) Composite of bandpass-filtered (7–20 years) MSLP anomalies (from 1911–1989 average) during wet austral winters in southwestern Australia. MSLP in hPa, with contours every 0.2 hPa. (b) Composite of bandpass-filtered (7–20 years) MSLP anomalies (from 1911–89 average) during dry austral winters in southwestern Australia. MSLP in hPa, with contours every 0.2 hPa. (c) Composite of bandpass-filtered (7–20 years) MSLP during wet austral winters in southwestern Australia. MSLP in hPa, with contours every 2 hPa. (d) Composite of bandpass-filtered (7–20 years) MSLP during dry austral winters in southwestern Australia. MSLP in hPa, with contours every 2 hPa. All of the diagrams were found to be field significant at the 99.9% level using Monte Carlo methods.

flow and a northward displacement of storm tracks over the Southern Ocean regions to the south-southwest of Australia. The converse is true of dry periods, when there is a westward expansion of the anticyclone, a lowering of MSLP in the trough, stronger zonal flow, and a southward shift in cyclone tracks over the Southern Ocean to the south-southwest of the continent. Some support for these findings is found in a comparison of patterns of Australian cyclonicity and anticyclonicity since the 1940s (Leighton and Deslandes 1991). A cyclonicity maximum affecting southwestern Western Australia dominated the circulation in the 1946–60 period, but is absent from the more recent 1965–87 analysis. Although this feature may be an artifact of poor observational data prior to the advent of regular weather satellite sensing of the higher latitudes of the Southern Hemisphere, it is an interesting finding in the light of the decadal–multidecadal circulation patterns discussed in this paper.

Further examination of the high-latitude trough to the southwest of Western Australia and upstream circulation features has been undertaken using MSLP data since 1957 at stations around the Antarctic coast, from Halley Bay (26.7°W, 75.5°S) to Dumont d'Urville (140.0°E, 66.7°S) (Fig. 8). Although based on a much shorter dataset, the smoothed time trace of MSLP around the Antarctic continent shows strong persistence in the location, but pronounced fluctuations in the intensity of the trough to the southwest of Western Australia (near the station at Casey at 110.5°W). In fact, the trough deepens to pressures below 985 hPa between 1966–71 and 1975–89 and becomes shallow with pressures above 985 hPa between 1957–65 and 1972–74. These periods coincide broadly with drier and wetter episodes in southwestern Australian austral winters and with fluctuations in the continental anticyclone discussed above. Farther to the west, in the longitudes of the Indian Ocean and southern Africa, the temporal structure is not as clear. There is some suggestion of a trough around 50°W, but in general the pattern is one of slightly higher-frequency MSLP fluctuations of the order of 7–10 years.

Overall, MSLP fields on decadal–multidecadal time scales tend to favor more northerly penetration of winter frontal systems over the southwest during wet pe-

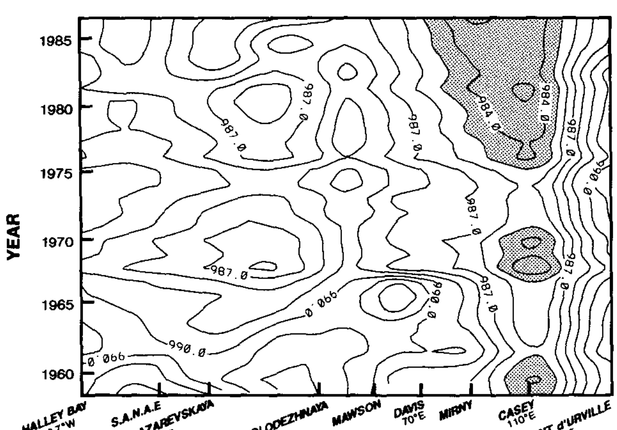

FIG. 8. Time plot of contoured and smoothed MSLP during austral winter (JJA) at Antarctic coastal stations from Halley Bay (26.7°W, 75.5°S) to Dumont d'Urville (140.0°E, 66.7°S) from 1958 to 1987. MSLP is in hPa, with contours every 1 hPa. The shaded region is where MSLP is less than or equal to 985 hPa.

riods and the converse occurs during dry periods. There is no apparent longitudinal shift in the southwest Australian trough between rainfall extremes. In fact, Wright (1974b) notes that, interannually, it is the least variable feature in the Southern Hemisphere circumpolar circulation and is a major control on blocking patterns in Australian–New Zealand longitudes.

c. Decadal–multidecadal signals in SST–rainfall and cloudiness–rainfall relationships

Bandpass-filtered SST anomaly fields are shown for composites of wet minus dry austral winters in Fig. 9. Regions of significant difference in SST using a gridpoint *t* test between the two composites are shaded. The overall field significance is greater than 99.9% using Monte Carlo methods. A coherent SST–rainfall pattern is evident in the wet-minus-dry winter composite. The most dominant feature is the presence of a warmer (colder) SST region across the southern Indian Ocean during dry (wet) seasons. From the earlier discussion of MSLP and circulation patterns, it is likely that this SST pattern is a consequence of reduced (increased) oceanic mixing and evaporation under the influence of easterly (westerly) wind anomalies during dry (wet) winters. A smaller area of warmer (colder) SST in wet (dry) winters is found to the northwest of the continent. This may provide a potential source of moisture for cloud bands in wet winters in southwestern Australia.

The broad pattern of alternating positive and negative SST anomalies in the western Indian Ocean off the Australian continent (Fig. 9), is similar in structure to patterns linked to winter rainfall over central eastern Australia in Nicholls (1989), Smith (1993), and Drosdowsky (1993). However, the major difference is that the distribution shown in Fig. 9 is one that would be associated with drier conditions over central eastern Australia in the above studies. Consequently, it is perhaps not surprising that the pattern in Fig. 9 does not quite resemble the pattern identified in Kuhnel (1990), who suggests that the warm SST region associated with cloud bands of the type likely to influence the southwest is usually found closer to northern Sumatra. The latter SST distribution may be responsible for the rainfall trend in districts immediately to the east-northeast of the southwestern region of Western Australia in Fig. 2.

Analyses of total cloudiness data since 1911 over the Indo-Australian region (Fig. 10) give a more "noisy" pattern for wet-minus-dry JJA composites. There is some evidence of slightly better organization in the spatial extent of cloud cover over and immediately to the west of Western Australia (as shown by the darker shaded area in Fig. 10), although this increase seems to be allied with the cooler SST region in Fig. 9. This data adds support to some degree of decadal–multidecadal modulation of rainfall processes over southwestern Australia via ocean–atmosphere interactions

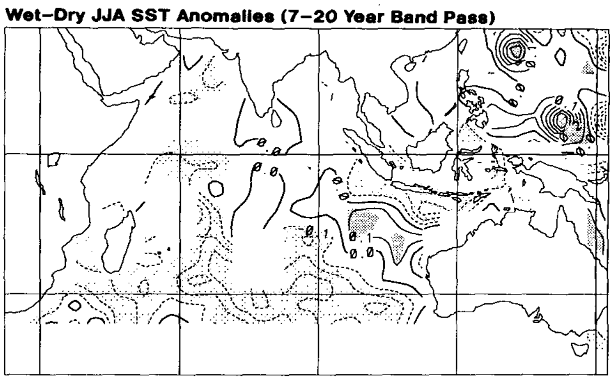

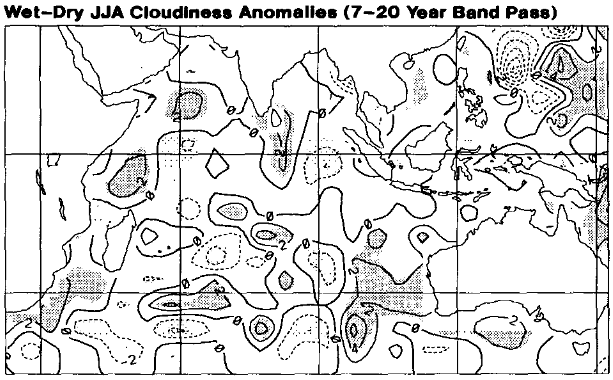

FIG. 9. Composite of bandpass-filtered (7–20 years) SST anomalies (from 1911–1989 average) for the difference between wet and dry (wet minus dry) austral winters in southwestern Australia. SST in °C, with contours every 0.1°C. Lightly shaded regions denote negative SST anomalies, darker shaded areas denote positive SST anomalies that are point significant at the 95% level. This difference composite is field significant at the 99.9% level using Monte Carlo methods.

FIG. 10. Composite of bandpass-filtered (7–20 years) cloudiness anomalies (from 1911–1989 average) for the difference between wet and dry (wet minus dry) austral winters in southwestern Australia. Cloudiness in percent of sky covered, with contours every 2%. Lightly shaded regions denote negative cloudiness anomalies, darker shaded areas denote positive cloudiness anomalies that are point significant at the 95% level. This difference composite is field significant at the 99.9% level using Monte Carlo methods.

involving tropical SSTs and cloud bands. However, it is not in the distinct configuration discussed in the references above.

d. Long-term trends in MSLP–rainfall relationships

Results of a low-pass filtering of gridded MSLP anomalies over the Australian region are shown for decadal intervals since 1911 in Fig. 11a. The most striking aspect of these diagrams is the contrasting MSLP anomalies over south-southwestern Australia and in the New Zealand region. This pattern changes through time, beginning with two MSLP centers of opposite sign in a negative/positive configuration (negative over Australia, positive near New Zealand) and progressing to a sequence that shows a positive/neg-

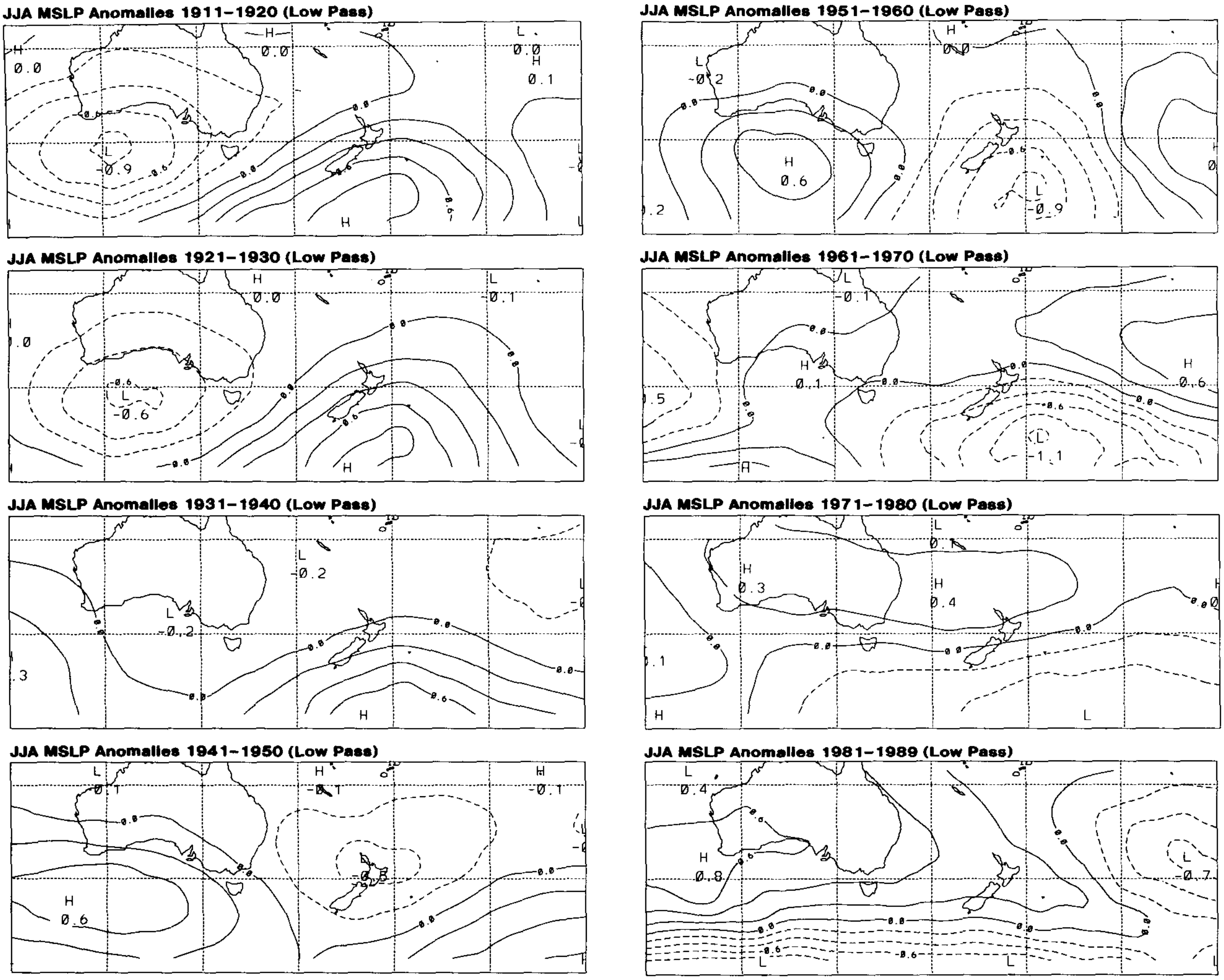

FIG. 11(a). Decadal means of low-pass-filtered (greater than 25 years) MSLP anomalies during JJA from 1911–1989. MSLP in hPa, with contours every 0.2 hPa.

ative alignment (positive over Australia, negative near New Zealand). Such patterns are strongest in the configuration of negative (positive) MSLP over south-southwestern Australia and positive (negative) MSLP near New Zealand in the 1911–30 (1941–1960) period. These changes are broadly consistent with a decrease in westerly zonal flow as described by Wright (1971 1974a,b) (his Type 2 category). Since 1971, the tendency is for a broad, positive MSLP anomaly to have developed over Australian longitudes. However, the 1981–1989 pattern is likely to be influenced by the strong decadal–multidecadal signal, as the low-pass filtering is unable to resolve the low-frequency signal toward the end points of the series. Thus, examination of data up to 1980 suggests that the magnitude of MSLP anomalies in Figs. 7a,b and 11a would have worked to suppress the decadal–multidecadal influence of low-MSLP anomaly episodes indicative of wet winters, and enhanced the high-MSLP–dry winter sequence. However, there is no evidence that this long-term MSLP signal is indicative of the enhanced greenhouse effect. In fact, an examination of the 2 × CO_2 MSLP simulations in intercomparisons of low- and high-resolution general circulation models (GCMs) (Whetton and Pittock 1991; Whetton, 1992, personal communication) fails to detect either the long-term or decadal–multidecadal MSLP patterns discussed in this paper.

Figure 11b shows low-pass-filtered MSLP in the region for decadal intervals since 1911. These diagrams suggest that an increase in the central pressure of the winter anticyclone over the Australian continent has occurred in the last two decades (since 1971). In addition, there is perhaps a slight tendency for a westward expansion of the anticyclone through the sequence shown. However, this is not nearly as pronounced as in the decadal–multidecadal results. Interestingly, none of the MSLP fields examined in this study show any indication of a distinct latitudinal shift in the winter

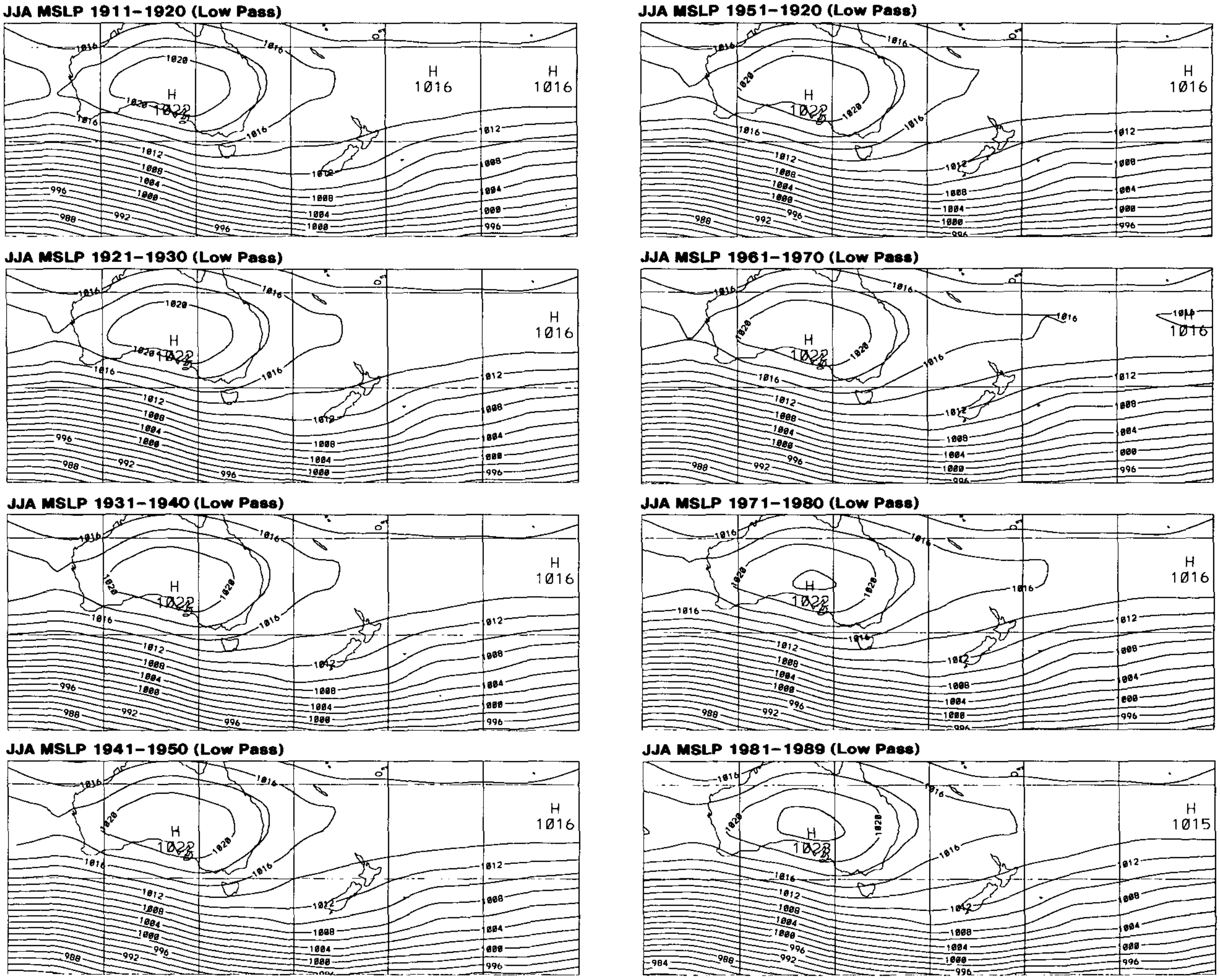

FIG. 11(b). Decadal means of low-pass-filtered (greater than 25 years) MSLP during JJA from 1911–1989. MSLP in hPa, with contours every 2 hPa.

anticyclone with rainfall extremes in southwestern Australia, as suggested by Wright (1971, 1974a,b).

e. Long-term trends in SST–rainfall and cloudiness–rainfall relationships

Only the overall linear trends in SST and cloudiness anomalies are shown in Figs. 12 and 13 (decadal patterns were calculated but show no more information). These fields are found to be 99.9% field significant. Nevertheless, the SST distribution (Fig. 12) is very different from the SST structure in the Indian Ocean resolved by the 7–20-year bandpass filtering of gridded SST data (Fig. 9). In general, there is a broad tendency for increased SST over the analysis period. Most structure is found in the southern Indian Ocean, where a band of increasing SSTs since 1911 extends from southern Africa to southern Australia. This feature is very similar to that observed in low-frequency analyses of ocean–atmosphere interactions in the Indian Ocean during austral summers (JFM) by Allan and Lindesay (1991) and Lindesay and Allan (1992). The sharp gradient in SST in the far southern Indian Ocean may reflect the gradient in ship observations and ship track densities noted in Bottomley et al. (1990).

A similar pattern is found in the low-pass-filtered cloudiness data (Fig. 13), although it is considerably noisier. The trend in cloudiness anomalies since 1911 is also one of a general increase in the Indo–Australasian region. Using an independent Australian Bureau of Meteorology cloudiness dataset, P. A. Jones (1991) and Jones and Henderson-Sellers (1992) have suggested that there has been a broad 5% increase in cloud amount over Australia between 1911 and 1989. Interestingly, P. A. Jones (1991) finds a significant positive correlation with the Southern Oscillation index (SOI) across the eastern half of the continent, but an insignificant relationship over the southwestern portion of

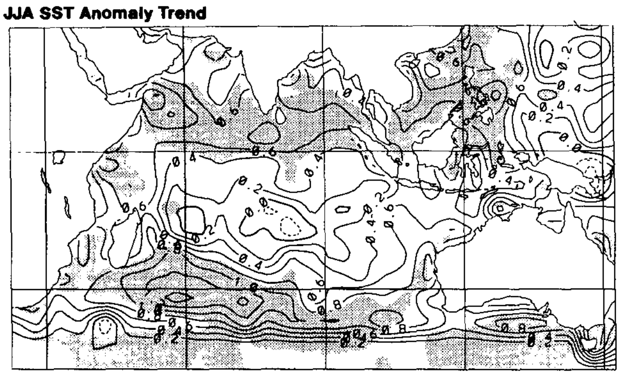

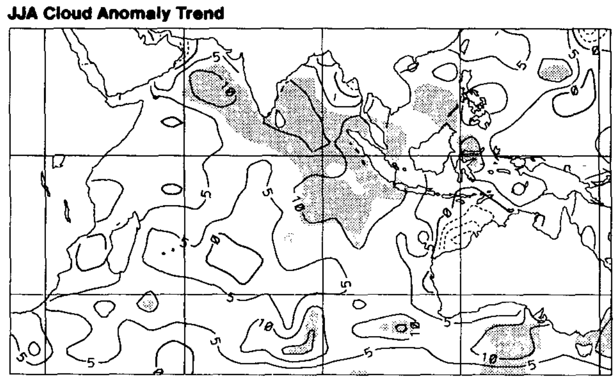

FIG. 12. Trend in SST anomalies during JJA from 1911–1989. SST in °C/100 years, with contours every 0.2°C. Regions of field significance at the 99.9% level are shaded.

FIG. 13. Trend in cloudiness anomalies during JJA from 1911 to 1989. Cloudiness in %/100 years, with contours every 5%. Regions of field significance at the 99.9% level are shaded.

Western Australia. In Fig. 13, the most coherent feature appears to be a broad area showing an increase in cloudiness over the northeastern Indian Ocean–Asian sector. However, it should be remembered that the COADS cloudiness data has not been subjected to the rigorous checking and corrections that have been applied to the UKMO SST observations used in this study.

f. Low-frequency ENSO influence

As noted earlier in this study, ENSO relationships with southwestern Australian rainfall based on data over the last 50–60 years are poor. However, given the MSLP–rainfall links at low frequencies discussed above and claims of significant correlations with the SOI for early and late winter rainfall (MJJ and ASO) in the period 1902–1965 by Wright (1974b) (MJJ $r = 0.30$; ASO $r = 0.35$; $p < 5\%$), it is useful to reexamine such correlations with data from 1876–1989. As studies have shown a strong relationship between the SOI and Darwin MSLP (Wright 1989; Zhang and Casey 1992), southwestern rainfall correlations are examined with both of these ENSO indices.

A 21-year sliding correlation analysis was used to examine links involving raw, linearly detrended, and low-pass filter-removed (components greater than 25 years) SOI and Darwin MSLP series with southwestern Australian rainfall since 1876 (Fig. 14). Removal of any linear trend or low-frequency component from the SOI or Darwin MSLP series failed to influence the resulting correlation pattern with southwestern Australian rainfall. Consequently, only the correlations with Darwin MSLP are shown here.

The sliding correlation analysis in Fig. 14 shows that significant correlations with southwest rainfall in midwinter to early spring are dominant from the beginning of records through to the 1930–40s. Since then, the negative correlation has weakened substantially and no coherent and significant link exists. Such changes may explain why the relationships of Perth MSLP and drought in Western Australia to the SOI were strong in the major 1877–78 ENSO, but not during the recent and slightly more severe 1982–83 event in the historical SOI analysis of Allan et al. (1991). Thus, Fig. 14 is perhaps suggestive of a low-frequency forcing in the climate system that affects ENSO characteristics by modulating the large-scale circulation regime in which the phenomenon operates. Resolution of this question is beyond the scope of this paper, but highlights the need for a better understanding of how ENSO operates and is modulated by the large-scale circulation under different historical climatic regimes.

4. Conclusions

In this study, circulation features responsible for the observed decrease in austral winter (JJA) rainfall over southwestern Australia have been proposed. In general,

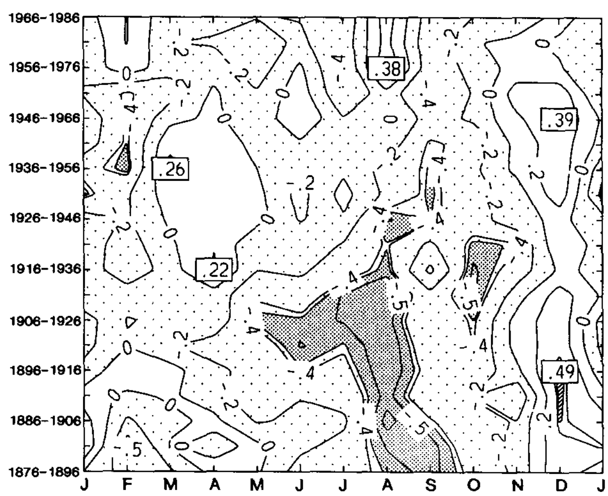

FIG. 14. 21-year sliding monthly correlations between Darwin MSLP and southwestern Australian rainfall since 1876. Areas of negative correlation are stippled, with the heaviest stippling denoting correlations significant at the 95% level. Positive correlations above the 95% significance level are crosshatched.

the most coherent and significant signals are seen in analyses of broad regional MSLP fields, which are suggestive of major fluctuations in circulation patterns. Though presenting a less clear picture, SST and cloudiness data do more to reinforce than contradict MSLP findings. Preliminary investigations also suggest that the relationship between ENSO and southwestern Australian winter rainfall has changed through time. Such patterns give further credence to indications that the ENSO phenomenon is responsive to low-frequency fluctuations.

From a local perspective, Perth MSLP shows a significant inverse correlation with southwestern Australian rainfall during JJA over the last 115 years. Periods of both lower (higher) MSLP and higher (lower) rainfall have been seen in this analysis, and a downward trend in rainfall is prevalent over the last 50 to 60 years. Gridded MSLP fields over Australasia indicate that the relationship is broader, with austral winter rainfall in southwestern Australia inversely correlated with local and regional MSLP patterns. Further investigations show that these MSLP–rainfall relationships involve a decadal–multidecadal (7–20 years) signal that is embedded in a longer-term (greater than 25 years) fluctuation. The latter is dominated by a pronounced decreasing (increasing) trend in rainfall (MSLP) since the mid-1960s.

An analysis of the decadal–multidecadal pulses has revealed that they are part of major circulation fluctuations in the region. During composites of dry (wet) winters, this involves a westward expansion (eastward contraction) and increase (decrease) in the central MSLP of the anticyclone over the Australian continent, and a decrease (increase) in MSLP in the longwave trough to the south-southwest of the Australian continent. Such analyses have also revealed the presence of more easterly (westerly) wind anomalies over southwestern Australia during dry (wet) season composites. In addition, these rainfall extremes appear to be linked to circulation changes involving interactions between SST anomalies over waters to the west of Australia and cloudiness patterns. It would seem that these changes are symptomatic of a modulation of midlatitude frontal systems, which results from fluctuations in the continental anticyclone and the semipermanent long-wave trough at higher latitudes.

Low-pass-filtered analyses of MSLP reveal the presence of a long-term, low-frequency signal in MSLP–rainfall relationships. Spatially, the MSLP pattern is dominated by a sequence that begins with low (high) anomalies over the southern Australian (in the New Zealand) region and ends with the opposite configuration. This slowly evolving feature may be indicative of the passage of a low-frequency wave that could provide a modulation of the long-wave pattern in this sector. Certainly, the decrease in southwestern Australian JJA rainfall appears to be the result of the development of positive MSLP anomalies over southern Australia under the influence of this low-frequency signal. Superimposed on this are the negative and positive MSLP pulses caused by the decadal–multidecadal feature. The phasing of these two signals works to suppress or enhance the rainfall trend. Increasing positive anomalies in SST and cloudiness patterns in the low-pass analysis are suggestive of a broad trend that is most coherent across the midlatitudes of the Indian Ocean and into southern Australian longitudes.

Neither the long-term, low-frequency or the decadal–multidecadal MSLP fields detailed in this study match the MSLP simulations under enhanced greenhouse conditions in current low- or high-resolution GCMs. However, there is further evidence that southwestern Australian rainfall has experienced low-frequency changes in its relationship to the ENSO phenomenon. Thus, it is evident that more research is required to ascertain the extent of the spatial influence of decadal–multidecadal, low-frequency, and long-term ENSO forcings on rainfall patterns.

Acknowledgments. This study was undertaken as part of an agreement with the Western Australian State Government, to provide ongoing scientific assessments of possible regional climatic impacts associated with global warming in the Western Australian region. We would like to thank Dr. J. L. Evans, Dr. R. L. Hughes, Dr. I. N. Smith, and Dr. A. B. Pittock of CSIRO, Division of Atmospheric Research, and Dr. J. A. Lindesay of the Climatology Research Group, University of Witwatersrand for their constructive comments on the initial manuscript. Gridded MSLP data were kindly provided by Dr. P. D. Jones, Climatic Research Unit, University of East Anglia.

REFERENCES

Allan, R. J., 1988: El Nino Southern Oscillation influences in the Australian region. *Prog. Phys. Geogr.*, **12**, 313–348.

——, 1989: ENSO and Climatic Fluctuations in Australasia. T. H. Donnelly and R. J. Wasson, Eds., *CLIMANZ III Proceedings of Symposium,* University of Melbourne, 49–61. [Available from the CSIRO Division of Water and Land Resources, P.O. Box 1666, Canberra, ACT, 2601, Australia.]

——, 1991: Australasia. *ENSO Teleconnections Linking Worldwide Climate Anomalies: Scientific Basis and Societal Impacts.* M. Glantz, R. Katz, and N. Nicholls, Eds., Cambridge University Press, 73–120.

——, 1993: Variations in ENSO and teleconnection structure. *27th International Geographical Congress, Proc. of the Commission on Climatology,* J. Arnfield, Ed., in press.

——, and J. A. Lindesay, 1992: Modulation of summer rainfall in southern Africa and Australia with teleconnection patterns across the Indian Ocean. *Int. Conf. on the Physical Causes of Drought and Desertification,* B. G. Hunt, Ed., Melbourne University (AMOS Publication 7).

——, K. Beck, and W. M. Mitchell, 1990: Sea level and rainfall correlations in Australia: Tropical links. *J. Climate,* **3,** 838–846.

——, N. Nicholls, P. D. Jones, and I. J. Butterworth, 1991: A further extension of the Tahiti–Darwin SOI, early ENSO events and Darwin pressure. *J. Climate,* **4,** 743–749.

——, C. D. Mitchell, and A. B. Pittock, 1992: *The greenhouse effect—Regional implications for Western Australia, annual report 1990–*

91. CSIRO Division of Atmospheric Research, 72 pp. [Available from the Climate Impact Group, CSIRO Division of Atmospheric Research, PMB No 1, Mordialloc, 3195, Victoria, Australia.]

Barnett, T. P., and P. D. Jones, 1992: Intercomparison of two different Southern Hemisphere sea level pressure datasets. *J. Climate,* **5,** 93–99.

Bottomley, M., C. K. Folland, J. Hsiung, R. E. Newell, and D. E. Parker, 1990: *Global Ocean Surface Temperature Atlas (GOSTA),* Meteorological Office and Massachusetts Institute of Technology, 20 pp.

Broadbridge, L., 1989: Climatic Change. Lowe, G., Ed., *Greenhouse 88, Planning for Climate Change, Western Australian Conference Proceedings,* Perth, WAWRC, 29–33. [Available from the Western Australian Water Resources Council, John Tonkin Water Centre, 629 Newcastle Street, Leederville, Western Australia, 6007, Australia.]

Cooke, W. E., 1901: *Climate of Western Australia from observations Made during the years 1876–1899.* Government Printer, 35 pp.

Drosdowsky, W., 1993: A method of forecasting winter rainfall over southern and eastern Australia. *Aust. Meteorol. Mag.,* in press.

Elliott, W. P., and J. K. Angell, 1988: Evidence for changes in Southern Oscillation relationships during the last 100 years. *J. Climate,* **1,** 729–737.

Enfield, D. B., 1988: Is El Nino becoming more common? *Oceanogr. Mag.,* **1, 2,** 23–27, 59.

——, 1989: El Nino, past and present. *Rev. Geophys.,* **27, 1,** 159–187.

——, and L. S. Cid, 1991: Low-frequency changes in El Niño–Southern Oscillation. *J. Climate,* **4,** 1137–1146.

Gentilli, J., Ed., 1971: *Climates of Australia and New Zealand, World Survey of Climatology, Volume* **13,** Elsevier Publishing Company, 405 pp.

——, 1979: Epitropical westerly jet advected storms. *Queensl. Geogr. J.,* **5,** 1–20.

Graham, R. J., 1963: Determination and analysis of numerical smoothing weights. *NASA* **TR-R-179,** 28 pp. [Available from NASA, Washington, DC 20546.]

Hunt, H. A., 1929: *Results of Rainfall Observations made in Western Australia.* Commonwealth Government Printer, 387 pp.

Jones, P. A., 1991: Historical records of cloud cover and climate for Australia. *Aust. Meteorol. Mag.,* **39,** 181–189.

——, and A. Henderson-Sellers, 1992: Historical records of cloudiness and sunshine in Australia. *J. Climate,* **5,** 260–267.

Jones, P. D., 1991: Southern Hemisphere sea level pressure data: An analysis and reconstructions back to 1951 and 1911. *Int. J. Climatol.,* **11,** 585–607.

——, and T. M. L. Wigley, 1988: Antarctic gridded sea level pressure data: An analysis and reconstruction back to 1957. *J. Climate,* **1,** 1199–1220.

Kidson, J. W., 1988: Interannual variations in the Southern Hemisphere circulation. *J. Climate,* **1,** 1177–1198.

Kuhnel, I., 1990: Tropical–extratropical cloudbands in the Australian region. *Int. J. Climatol.,* **10,** 341–364.

Lavery, B., A. Kariko, and N. Nicholls, 1992: A historical rainfall data set for Australia. *Aust. Meteorol. Mag.,* **40,** 33–39.

Leighton, R. M., and R. Deslandes, 1991: Monthly anticyclonicity and cyclonicity in the Australasian region: Averages for January, April, July and October. *Aust. Meteorol. Mag.,* **39,** 149–154.

Lindesay, J. A., and R. J. Allan, 1992: Teleconnection patterns across the Indian Ocean and summer rainfall in Australia and southern Africa. *Technical Programme Abstracts of the 27th Int. Geographical Congress,* Washington, 372 pp.

Lockyer, N., 1908: *Monthly Mean Values of Barometric Pressure for 73 Selected Stations Over the Earth's Surface.* Solar Physics Committee, 97 pp.

Lockyer, W. J. S., 1909: *A Discussion of Australian Meteorology.* Solar Physics Committee, 117 pp.

National Climate Centre, 1988: *Seasonal Outlooks (Based on El Nino/Southern Oscillation (ENSO) Relationships).* Bureau of Meteorology, Melbourne, 34 pp. [Available from the National Climate Centre, Bureau of Meteorology, GPO Box 1289K, Melbourne, 3001, Victoria, Australia.]

Nicholls, N., 1989: Sea surface temperatures and Australian winter rainfall. *J. Climate,* **2,** 965–973.

——, and B. Lavery, 1992: Australian rainfall trends during the twentieth century. *Int. J. Climatol.,* **12,** 153–163.

Parker, D. E., 1987: The Meteorological Office historical sea surface temperature data set. *Meteorol. Mag.,* **116,** 250–254.

Pittock, A. B., 1975: Climatic change and the patterns of variation in Australian rainfall. *Search,* **6,** 498–504.

——, 1983: Recent climatic change in Australia: Implications for a CO_2 warmed earth. *Clim. Change,* **5,** 321–340.

——, 1988: Actual and anticipated changes in Australia's climate. Pearman, G. I., Ed., *Greenhouse: Planning for Climate Change.* CSIRO/Aust. Acad. Science/Cambridge Uni Press, 35–53.

——, and R. J. Allan, (Eds.), 1990: *The greenhouse effect: Regional implications for Western Australia, 1st Interim report 1989–90.* Environmental Protection Authority, 65 pp. [Available from the Climate Impact Group, CSIRO Division of Atmospheric Research, PMB No 1, Mordialloc, 3195, Victoria, Australia.]

Reseau Mondial, 1910–34: *British Meteorological and Magnetic Year Book Part* **V.** H. M. Stationary Office.

Sadler, B. S., G. W. Mauger, and R. A. Stokes, 1988: The water resource implications of a drying climate in south-west Western Australia. Pearman, G. I., Ed., *Greenhouse: Planning for Climate Change,* CSIRO/Aust. Acad. Science/Cambridge Uni Press, 296–311.

Smith, I., 1993: The potential for an improvement in the predictability of Australian seasonal rainfall using sea surface temperatures. *Int. J. Climatol.,* in press.

Smithsonian Institute, 1944: World weather records. *Smithsonian Miscellaneous Collections, Vol 79,* Smithsonian Institute, 1199 pp.

Stearns, S. D., and D. R. Hush, 1990: *Digital Signal Analysis.* Prentice-Hall, 440 pp.

Tapp, R. G., and S. L. Barrell, 1984: The north-west Australian cloud band: climatology characteristics and factors associated with development. *J. Climatol.,* **8,** 155–177.

Whetton, P. H., and A. B. Pittock, 1991: Australian Region Intercomparison of the Results of Some General Circulation Models used in Enhanced Greenhouse Experiments. CSIRO Division of Atmospheric Research Technical Paper No. 21, 73 pp. [Available from the Climate Impact Group, CSIRO Division of Atmospheric Research, PMB No 1, Mordialloc, 3195, Victoria, Australia.]

Woodruff, S. D., R. J. Slutz, R. L. Jenne, and P. M. Steurer, 1987: A comprehensive ocean–atmosphere Data Set. *Bull. Amer. Meteor. Soc.,* **68,** 1239–1250.

Wright, P. B., 1971: Spatial and temporal variations in seasonal rainfall in south-western Australia. Miscellaneous Publication 71/1, Institute of Agriculture, University of Western Australia, Agronomy Department, 89 pp.

——, 1974a: Seasonal rainfall in southwestern Australia and the general circulation. *Mon. Wea. Rev.,* **102,** 219–232.

——, 1974b: Temporal variations in seasonal rainfalls in southwestern Australia. *Mon. Wea. Rev.,* **102,** 233–243.

——, 1989: Homogenized long-period Southern Oscillation indices. *J. Climatol.,* **9,** 33–54.

Zhang, X. G., and T. M. Casey, 1992: Long Term Variation of the Southern Oscillation and Relationships with Australian rainfall. *Aust. Meteorol. Mag.,* **40,** 211–225.